

# INSIGHTS INTO FORMATION OF Nb<sub>3</sub>Sn FILM DURING THE VAPOR DIFFUSION PROCESS\*

Uttar Pudasaini<sup>1</sup>, G. Ereemeev<sup>2</sup>, Charles E. Reece<sup>2</sup>, J. Tuggle<sup>3</sup>, and M. J. Kelley<sup>1,2,3</sup>

<sup>1</sup>Applied Science Department, The College of William and Mary, Williamsburg, VA 23185, USA

<sup>2</sup>Thomas Jefferson National Accelerator Facility, Newport News, VA 23606, USA

<sup>3</sup>Virginia Polytechnic Institute and State University, Blacksburg, VA 24061, USA

## Abstract

The potential of Nb<sub>3</sub>Sn for superconducting radio frequency (SRF) cavities is widely recognized and renewed R&D efforts continue to bring new insights about the material's structure and properties. We have systematically coated niobium with Nb<sub>3</sub>Sn using the vapor diffusion technique under varying coating conditions to elucidate the reaction of tin with niobium at the temperatures of interest. The analysis of the coated samples is revealing new understanding about the two-stage nucleation/deposition ("vapor diffusion") process that allows us to form a hypothesis regarding Nb<sub>3</sub>Sn formation mechanism. The essential aspect of nucleation is the deposition of a high coverage, nanoscale-thin tin film with particle assemblage by decomposition of tin chloride on the niobium surface at temperatures sufficient for reduction of the thick niobium oxide film, usually at about 500 °C. The deposition is followed by the reaction of tin from tin vapor with the niobium surface to form Nb<sub>3</sub>Sn at about 1200 °C, where the surface and grain boundaries start to play key role in the formation process initiation and progression. These findings improve understanding of the Nb<sub>3</sub>Sn growth in the typical vapor diffusion process used for accelerator cavity coatings

## INTRODUCTION

Since the performance of niobium SRF cavities is now approaching the fundamental limit, SRF technology based on alternate superconducting materials is gaining more attention for better performance and cost reduction. The alternative SRF cavity material demands higher values of both the critical temperature and superheating field because they determine the RF performance and accelerating gradient of SRF cavity. The intermetallic compound Nb<sub>3</sub>Sn pledges better performance and significant reduction of production and operational cost of SRF cavities, because both the critical temperature and superheating field of Nb<sub>3</sub>Sn are nearly twice that of niobium [1]. At the present time, it is the front running alternative material to substitute niobium in SRF cavities. Because of the brittleness and lower thermal conductivity of bulk material, Nb<sub>3</sub>Sn cavities should be prepared by depositing a thin layer of Nb<sub>3</sub>Sn coating inside a prefabricated cavity structure. Tin vapor diffusion is the leading technique for coating the interior surface of a

niobium cavity with a Nb<sub>3</sub>Sn layer of few-micron thickness.

The tin vapor diffusion technique is comprised of two steps—nucleation and deposition. The nucleation step involves tin chloride evaporation at a lower temperature of about 500 °C. Deposition follows nucleation, and involves evaporation of tin at a higher temperature of 1100 - 1200 °C, a temperature favorable to form Nb<sub>3</sub>Sn phase on substrate niobium. Since the performance of a Nb<sub>3</sub>Sn-coated cavity prepared by this technique is very promising, it is necessary to better understand the mechanism of Nb<sub>3</sub>Sn formation and its growth kinetics to optimize the coating parameters for further improvement. This contribution discusses the results from recent experiments that could shed some new light on the formation and kinetics of Nb<sub>3</sub>Sn coating during the coating process.

## Nb<sub>3</sub>Sn COATING EVOLUTION

The typical coating process at Jefferson Lab consists of a 1-hour nucleation step at 500 °C followed by a 3-hour deposition step at 1200 °C [2]. A set of scanning electron microscopy (SEM) images is shown in Figure 1 to elucidate the evolution of a Nb<sub>3</sub>Sn coating.

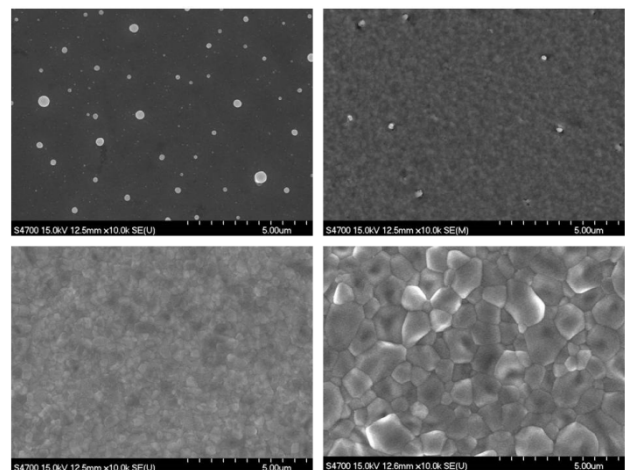


Figure 1: SEM images obtained after interrupting the coating process after one hour at 500 °C (top left), one minute at 1200 °C (bottom left), one hour at 1200 °C and 3 hours at 1200 °C (bottom right). Note that similar amounts of Sn and SnCl<sub>2</sub> were used in each experiment.

\*Partially authored by Jefferson Science Associates under contract no. DEAC0506OR23177. Work at College of William & Mary supported by Office of High Energy Physics under grant SC0014475. This material is based upon work supported by the U.S. Department of Energy, Office of Science, Office of Nuclear Physics.

Content from this work may be used under the terms of the CC BY 3.0 licence (© 2017). Any distribution of this work must maintain attribution to the author(s), title of the work, publisher, and DOI.

surface following the end of nucleation step at 500 °C. The formation of grains with sizes on the order of a few tenths of nanometers is evident as soon as the temperature reaches to 1200 °C. Grain growth is significant at the deposition temperature. The grain size reaches a few hundreds of nanometers after one hour and about one micron over the next two hours.

Samples obtained after one hour of nucleation were subjected to supplementary analysis with X-ray photoelectron spectroscopy (XPS) and scanning Auger microscopy (SAM). Although the exact mechanism its formation is not yet understood, it is clear from XPS and SAM analysis that a nanoscale-thin tin film with coverage of evenly distributed tin particles formed on the niobium substrate surface [3] (see Fig. 2).

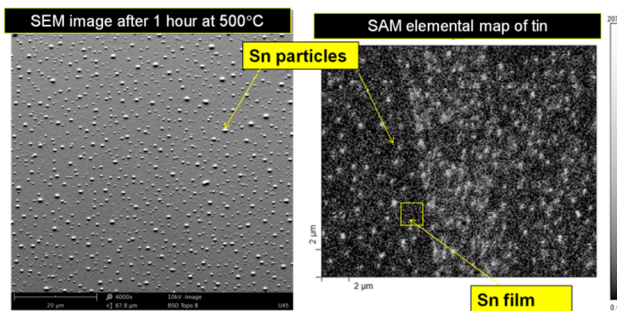


Figure 2: SEM image (left) and SAM (right) obtained from the sample treated for 1 hour at 500 °C. Note that SAM reveals a nanoscale-thin tin film.

To understand how the coating formation proceeds after the nucleation step, an “overcoat” experiment was performed. Details of experiment and characterization results are presented in next section.

## OVERCOAT EXPERIMENT

A number of previously coated Nb<sub>3</sub>Sn samples were subjected to a second coating, or overcoating, with a similar experimental setup. The temperature profile followed was similar to the profile used in the standard coating procedure, but no SnCl<sub>2</sub> was used in this experiment. A summarized description of experimental samples prior to the second coating, along with grain sizes before and after the second coating, are presented in Table 1. Samples chosen for overcoating originated from several different experimental runs that produced Nb<sub>3</sub>Sn coatings with a variety of grain sizes and notable surface features. Each sample was subjected to SEM/EDS analysis before and after the overcoating experiment. A few selected samples were also examined with atomic force microscopy (AFM) and electron backscatter diffraction (EBSD) analysis. Details of EBSD examination are available in [4].

SEM images of a few samples before and after the experiment are shown in Figure 3. Table 1 shows that overcoating apparently induced an increase in the Nb<sub>3</sub>Sn grain size for each sample. The average grain size for each sample before and after overcoating was calculated from SEM images. A grain size increase factor was

determined for each sample by taking the ratio of the average grain size after and before the experiment. There appears to be a correlation between the grain size increase factor and the grain size prior to overcoating. It is seen that the grain size in niobium sample coated in overcoat experiment (with Sn only) is smaller than any of the pre-coated samples included in the same run. AFM images obtained from overcoated samples shows residue a few nanometers in size. We suspect this is unreacted tin.

Table 1: Description of Samples Used in Overcoat Experiment

Sample	Description of sample before coating	Average grain size before coating (μm <sup>2</sup> )	Average grain size after coating (μm <sup>2</sup> )	Grain size increase factor
U144	pre-coated Nb <sub>3</sub> Sn with 400 °C nucleation, low Sn experiment	0.8	2.3	2.88
U129	pre-coated Nb <sub>3</sub> Sn with standard coating	1.2	2.3	1.92
U105	pre-coated Nb <sub>3</sub> Sn with standard coating	1.3	2.4	1.85
U91	pre-coated Nb <sub>3</sub> Sn with 450°C nucleation	1.7	2.8	1.65
U108	pre-coated Nb <sub>3</sub> Sn without SnCl <sub>2</sub>	2.1	3.3	1.14
U150	Nanopolished Nb		2.1	
U113	BCP treated Nb		1.8	

The cross section of an overcoated sample was examined by EBSD. The EBSD image shows additional grain formation in the Nb-Nb<sub>3</sub>Sn interface as shown in Figure 4b. This orientation image map (OIM) is different than that of a regular Nb<sub>3</sub>Sn coating, which normally exhibits columnar grains extending all the way from the top surface to the Nb-Nb<sub>3</sub>Sn interface [5]. It is clear that no new surface layer is grown during overcoating. Furthermore, grain growth appears to be faster next to Nb<sub>3</sub>Sn grain boundaries at the Nb-Nb<sub>3</sub>Sn interface, which can be seen as “cupping” at the base of many Nb<sub>3</sub>Sn grains as shown in Figure 4a. Due to these observations we are inclined to believe that grain boundary diffusion is the primary mode for Sn transport to the interface where grain growth proceeds. This finding appears to be consistent with SEM results of growth rate, which was found to vary inversely with pre-overcoated grain size, see Table 1.

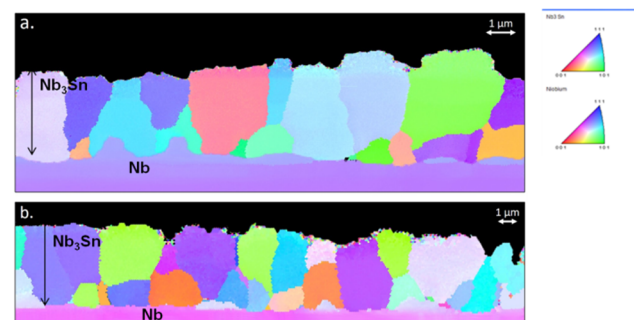


Figure 4: EBSD images obtained from overcoated sample U105. Approximate orientations of Nb<sub>3</sub>Sn and Nb grains are shown with inverse pole figure.

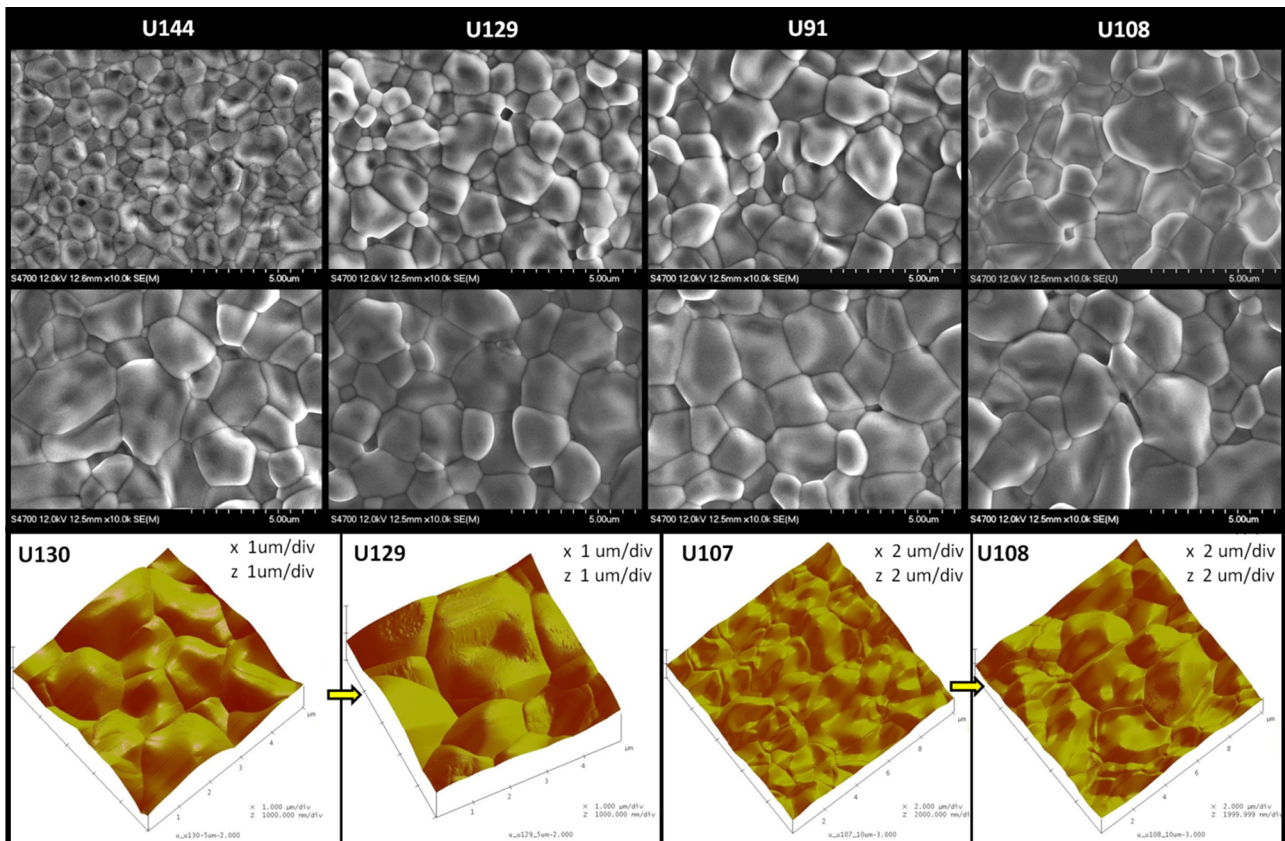


Figure 3: SEM images before and after the overcoat experiment. The last row of images (from left to right) are AFM images of U130 (before overcoat), U129 (after overcoat), U107 (before overcoat) and U108 (after overcoat). U130/U129 and U107/U108 were prepared identically in the same experimental runs. Note that some residues residues on overcoat samples.

### GROWTH OF PATCHY REGION

Patchy regions are thin film regions in the  $Nb_3Sn$  coating [6-8], and although they have been observed and reported by different researchers, the cause of their formation has not yet been established. One possible explanation is that patches form in areas where nucleation is not as profuse, so that  $Nb_3Sn$  particles may have grown laterally before coalescing. A SEM image of a patchy region found in sample U145, which appears smoother than the surrounding  $Nb_3Sn$  coating, is shown in Figure 5 (left). The corresponding EBSD image in Figure 5 (right) depicts patches as large single grains of  $Nb_3Sn$ . A cross section of a patchy region was also prepared with a focused ion beam (FIB), and was analyzed using SEM to quantify the thickness of the coating in such areas as shown in Figure 6. The patch thickness was measured to be  $194(\pm 59)$  nm, roughly an order of magnitude less than a well-coated area with measured thickness  $1.6(\pm 0.1)$   $\mu m$ . Note that the substrate of sample U145 was nanopolished, that is, the surface roughness is on the order of few nanometers. A cross-sectional image of the patchy region and corresponding EBSD image are shown in Figure 6. It shows that the bulk niobium below an unusually sparse  $Nb_3Sn$  coating is of greater thickness than the niobium on either side of the patch where “normal”  $Nb_3Sn$  coating is located. Since the starting substrate niobium sample

surface was uniformly smooth, this indicates that tin diffuses downward into the niobium bulk forming  $Nb_3Sn$  layer at the Nb interface, and subsequent grain growth progresses downward, consuming Nb as Sn is transported through the  $Nb_3Sn$ -Nb interface.

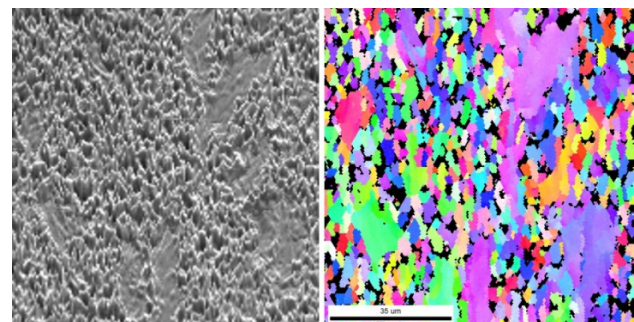


Figure 5: SEM image of a patchy area obtained in sample U145 (left) and an EBSD image from the same sample (right). Black areas in the EBSD image arise from a combination of  $Nb_3Sn$  grain topography and low electron beam incident angle (20 degree).

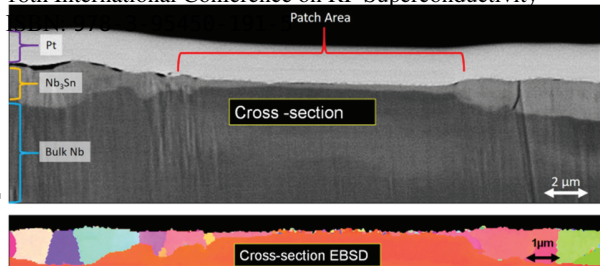


Figure 6: SEM image of FIB cross-section of patchy region (top) and corresponding EBSD image (bottom).

A rigorous investigation is required to determine the formation mechanism of patchy regions. However, considering the inverse relationship between the grain growth increase factor and grain size of the substrate, it is expected that large single crystalline grains of patchy area once it form may grow much more slowly than regular sized grains leading to thin film compared to thicker coating in neighboring regions. This is directly related to the low density of grain boundaries present in the patchy areas available to transport tin to the Nb-Nb<sub>3</sub>Sn interface for formation of additional Nb<sub>3</sub>Sn.

## CONCLUSION

Following a typical Nb<sub>3</sub>Sn coating process, we conducted surface studies of several samples prepared at different stages of the coating process. The essential function of the nucleation step appears to be the formation of a high coverage, nano-thin tin layer film or particle assemblage. This occurs through decomposition of tin chloride on the niobium substrate surface following the dissolution of a niobium pentoxide film at ~500 °C. Once the furnace temperature reaches ~1200 °C, tin reacts with niobium to form Nb<sub>3</sub>Sn particles covering the full surface, and the desired Nb<sub>3</sub>Sn coating ultimately evolves. Results from overcoat experiments indicate that tin primarily diffuses downward through grain boundaries at the Nb<sub>3</sub>Sn-Nb interface, resulting in growth of Nb<sub>3</sub>Sn that extends deeper and deeper into the Nb bulk. The growth starts to slow down with increasing grain size because of a decreasing density of grain boundaries. Similarly, the patchy region in Nb<sub>3</sub>Sn coating which contains large single crystalline grains is composed of a significantly thin coating because of only a few grain boundaries available for tin transport.

We are very thankful for Olga Trifimova at William and Mary Applied Research Center for her continuous help and support for AFM characterization. EBSD analysis was done at Nanoscale Characterization and Fabrication Laboratory (NCFL) at Virginia Tech.

## REFERENCES

- [1] D.B. Liarte, S. Posen, M.K. Transtrum, G. Catelani, M. Liepe and J.P. Sethna, "Theoretical estimates of maximum fields in superconducting resonant radio frequency cavities: stability theory, disorder, and laminates", *Superconductor Science and Technology*, vol. 30, no. 3, p. 033002, Jan 2017.
- [2] G. Ereemeev, M. Kelley, U. Pudasaini, C. Reece, and J. Tuggle. "Progress with multi-cell Nb<sub>3</sub>Sn Cavity development linked with sample materials characterization." In *17th International Conference on RF Superconductivity (SRF2015)*, Whistler, BC, Canada, Sept. 2015, pp. 505-511.
- [3] U. Pudasaini, G.V. Ereemeev, M.J. Kelley, and C.E. Reece, "Experimental Study of Nucleation for Nb<sub>3</sub>Sn Diffusion Coatings on Niobium SRF Cavities", in *Proc. 28th Linear Accelerator Conf. (LINAC'16)*, East Lansing, MI, USA, Sep. 2016, paper THOP01, pp. 740-743.
- [4] J. Tuggle, G.V. Ereemeev, M.J. Kelley, A.D. Palczewski, U. Pudasaini, and C.E. Reece, "Materials characterization for SRF cavities: gaining insight into Nb<sub>3</sub>Sn", in *Proc. 8th Int. Particle Accelerator Conf. (IPAC'17)*, Copenhagen, Denmark, May 2017, paper MOPVA114, pp. 1111-1114.
- [5] U. Pudasaini, G.V. Ereemeev, M.J. Kelley, C.E. Reece, and J. Tuggle, "Investigation of Structural Development in the two-step diffusion coating of Nb<sub>3</sub>Sn on niobium", in *Proc. North American Particle Accelerator Conf. (NAPAC'16)*, Chicago, IL, USA, Oct. 2016, paper WEB1CO02, pp. 659-662.
- [6] S. Posen and M. Liepe, in *Proc LINAC'14*, Geneva, Switzerland, 2014, paper TUIOC03.
- [7] Daniel Leslie Hall, J.J. Kaufman, M. Liepe, and J.T. aniscalco, "Surface analysis studies of Nb<sub>3</sub>Sn thin films", in *Proc. IPAC'16*, Busan, Korea, 2016, paper WEPMR023.
- [8] U. Pudasaini, G.V. Ereemeev, M.J. Kelley, C.E. Reece, and J. Tuggle, "Examination of Cutouts Inner Surfaces from Nb<sub>3</sub>Sn Coated Cavity", in *Proc. 28th Linear Accelerator Conf. (LINAC'16)*, East Lansing, MI, USA, Sep. 2016, paper MOPLR023, pp. 189-192.